PyCSFex: An extensible Python 3 package for calculating X-ray structure factors in complex crystals

John P. Sutter*[a], James Pittard[b], Jacob Filik[a], Alfred Q. R. Baron[c]
[a]Diamond Light Source Ltd, Harwell Science and Innovation Campus, Chilton, Didcot, OX11 0DE, United Kingdom
[b]School of Physics, HH Wills Physics Laboratory, University of Bristol, Tyndall Avenue, Bristol, BS8 1TL, United Kingdom
[c]Materials Dynamics Laboratory, RIKEN SPring-8 Center, 1-1-1 Kouto, Sayo, Hyogo 679-5148, Japan

ABSTRACT

Near-perfect diffracting crystals have many uses in X-ray optics including as monochromators, energy analyzers, and phase retarders. The usefulness of a particular Bragg reflection is often related to its angular acceptance and efficiency, as is determined by the reflection's structure factor. Silicon crystals, which belong to the same face-centered cubic space group $Fd\bar{3}m$ as germanium and diamond, are readily available in large and highly pure ingots. Combined with their high thermal conductivity and low thermal expansion, this makes them suitable for synchrotron X-ray beamlines. However, less symmetric trigonal crystals such as sapphire, lithium niobate, and α-quartz offer a better choice of high-energy-resolution Bragg reflections near backscattering with less likelihood of parasitic Bragg reflections. Because these crystals' atoms vibrate anisotropically and shift relative to each other with temperature, the temperature dependence of their structure factors is not a given by a simple Debye-Waller factor. Also, many crystal structures may be described by several different conventions of origin and lattice vectors. A Python 3 software package, PyCSFex, is presented here for the rapid calculation of large numbers of structure factors of any crystal described in any convention. It can run on its own or as part of an already existing software package. Users can extend the package to new crystals by writing their own material files. α-Quartz is chosen as an example because it has already been successfully used in backscattering X-ray energy analyzers and presents the complexities previously mentioned.

Keywords: X-ray, crystal, structure factor, Python, quartz

1. INTRODUCTION

For many years, X-ray beamlines at synchrotrons and free electron lasers have used silicon crystal optics because of the combination of highly favorable thermal, mechanical, and material properties that such crystals offer. Because silicon is a critical material for the manufacture of semiconductors, large ingots up to 125 mm in diameter and 1 m long with extremely low impurity and defect concentrations are regularly grown by industrial suppliers using the float-zone method. Silicon's high thermal conductivity[1] allows it to dissipate high thermal loads, and because its linear thermal expansion coefficient is zero[2] at 120 K, silicon crystals suffer relatively little distortion under such loads when cooled by liquid nitrogen. Silicon crystals are hard enough to take a high polish, yet they can still be cut and shaped by diamond saws, and after fabrication, surface damage can be removed by etching with aqueous mixtures of nitric and hydrofluoric acid. Finally, silicon crystal optics remain undamaged through years of operation. Therefore, silicon crystals are the preferred material for X-ray monochromators, especially those exposed to beams of high power.

Germanium and diamond crystals are also sometimes used as X-ray diffracting optics, though each has some disadvantages compared with silicon. Germanium absorbs X-rays more strongly, has a higher linear thermal expansion coefficient[2], and has lower thermal conductivity[1] than silicon. Nonetheless, germanium crystals are frequently used along with silicon crystals as high-resolution energy analyzers for measurements of X-ray fluorescence and inelastic scattering, which do not impose high thermal loads. Large and defect-free crystals of diamond are difficult to produce and also difficult to machine and etch. They are therefore unsuitable for making crystal energy analyzers. However, their low thermal expansion[3] and high thermal conductivity[4] make them attractive as filters for removing X-rays of energy < 5 keV, which at some beamlines are not used and would impose intolerable thermal loads on optics downstream. Moreover, their low absorption makes them the material of choice for phase retarders, which alter the polarization state of an X-ray beam and thus are useful for measurements of circular dichroism, as well as for multiplexing monochromators.

*john.sutter@diamond.ac.uk; phone 44 1235 778626; fax 44 1235 778784; www.diamond.ac.uk

Advances in Computational Methods for X-Ray Optics VI, edited by Oleg Chubar, Takashi Tanaka, Proc. of SPIE Vol. 12697, 126970A · © 2023 SPIE
0277-786X · doi: 10.1117/12.2676361

All three materials, silicon, germanium and diamond, form crystal structures whose symmetry operations are those of the face-centered cubic space group $Fd\bar{3}m$. The set of symmetry operations is remarkable for its large number of rotations, mirror planes, and glide planes, as well as for including inversion (that is, these materials are centrosymmetric)[5]. As a result, the number of atomic planes in these crystals that are related by symmetry and thus have the same spacing d is much larger than in crystals whose structures have fewer symmetry operations. This particularly affects the design of crystal energy analyzers, which achieve their best resolution if they diffract X-rays close to backscattering[6,7]. Since the energy of the X-rays to be analyzed is often fixed, for example at an emission line or absorption edge of some element, the likelihood that silicon and germanium can diffract those X-rays near backscattering is low. Furthermore, diffraction in backscattering from these materials is accompanied by parasitic reflections that remove the desired flux and affect the energy resolution. For instance, when the (12 4 0) atomic planes of silicon and germanium diffract in backscattering, 22 additional reflections are also excited[8]. For these reasons, non-cubic crystals that have fewer symmetry operations are being considered as possible materials for crystal energy analyzers of X-rays. Sapphire, lithium niobate, and α (or "low") quartz have attracted the most interest[9]; they are described in Table 1. All these form trigonal crystal systems. Note that although the space groups of sapphire and lithium niobate appear similar, they are quite different. The crystal structure of sapphire is centrosymmetric, whereas that of lithium niobate is polar. The latter is therefore ferroelectric while the former is not. It is also notable that α quartz is piezoelectric; as is possible because it is also non-centrosymmetric.

Table 1: Crystals with trigonal systems that are being considered for use as high-resolution X-ray energy analyzers. Names of space groups are as listed in the International Tables for Crystallography[5]. The two space groups in which the crystal structure of α quartz may exist are both chiral and are enantiomorphs (mirror images) of each other.

Crystal	Chemical formula	Space group	Lattice system
α quartz	SiO_2	$P3_121$ or $P3_221$	Hexagonal
Sapphire	Al_2O_3	$R\bar{3}c$	Rhombohedral
Lithium niobate	$LiNbO_3$	$R3c$	Rhombohedral

α quartz crystals synthetically grown by the hydrothermal process[10] are commercially available. Their low defect concentration has been demonstrated[11-14]. They have already been put to work as spherically diced analyzers for the Ni Kα emission line and the Ir L3 absorption edge[15,16] and as a flat crystal analyzer accompanied by a collimating Montel optic after the sample for the Ir L3 absorption edge[17]. In the last example, the energy resolution of the analyzer was estimated to be ~4 meV. Sapphire and lithium niobate crystals have also been tested, and although the samples currently available do not yet attain such a low concentration of defects[9], future specimens may benefit from improved fabrication methods. Therefore, the development of methods for determining the performance of these materials as crystal energy analyzers of X-rays will be well worth the effort. In the future other crystalline materials may find applications as X-ray optics, and these methods will have to be extended to include them. Finally, for ease of use, these methods should be readily integrated with currently existing software packages for X-ray optics simulations, such as *OASYS*[18] and *SRW*[19].

However, to achieve this goal, crystals more complex than silicon, germanium, and diamond will have to be treated. In general, their thermal expansion will be anisotropic, as will the thermally induced vibration of their atoms. In addition, whereas the relative positions of the atoms in silicon, germanium, and diamond are independent of temperature, the same is not true for all crystals. Because crystal X-ray energy analyzers are often tuned by deliberately varying their temperature, all these factors need to be considered if the analyzer's performance is to be predicted accurately.

A difficulty well known to crystallographers, but less so to many designers of X-ray optics, is that many crystal structures can be defined by multiple choices of origin and lattice vectors. A simple example is the choice between two possible coordinate origins for silicon, germanium, diamond, and other crystal structures belonging to the face-centered cubic space group $Fd\bar{3}m$. All these structures have a basis of two atoms separated by one-fourth of the body diagonal of the cubic unit cell. The origin may be placed either on the first atom of the basis or at the inversion center between the two atoms of the basis, and there is no universal agreement on which choice is better. For more complex crystal structures, the number of possible descriptions can be even greater, and though proposals for standardizing crystallographic data have been published[20,21], none has been completely adopted. α quartz is an extreme example that has been discussed at length[22-24].

The structure factors of a crystal's Bragg reflections are a critical parameter for the design of diffracting X-ray optics, and they depend on both the temperature and the atomic positions. A software package *PyCSFex* ("Python crystal structure

factor extensible") for calculating X-ray structure factors in any crystal while leaving users free to choose their preferred description of the crystal structure has recently been published[25]. It is available at https://github.com/DiamondLightSource/PyCSFex. Each crystal is described by a material file written by a user and processed by a set of core modules. Material files have been provided for silicon, germanium, diamond, and α quartz. The package is written entirely in Python 3 for easy integration with many already released software modules. Some less commonly discussed aspects of the theory on which *PyCSFex* is based are discussed below, with α quartz being used as an example.

2. THEORY

2.1 Definition of structure factors of crystals

Crystals are indispensable for studies of all types of materials because their long-range periodicity on scales comparable to X-ray wavelengths enables them to diffract X-rays with high efficiency provided Bragg's Law is fulfilled:

$$n\lambda = 2d \sin\theta\,, \tag{1}$$

where n is a positive integer giving the order of the diffraction, λ is the wavelength of the X-rays, d is the spacing of a particular set of parallel atomic planes in the crystal, and θ is the "Bragg angle" between the atomic planes and the X-ray beam. For every crystal one may define a set of lattice vectors **a**, **b**, and **c** from which reciprocal lattice vectors **a***, **b***, and **c*** can be determined:

$$\mathbf{a^*} = \frac{\mathbf{b}\times\mathbf{c}}{\mathbf{a}\cdot\mathbf{b}\times\mathbf{c}};\ \mathbf{b^*} = \frac{\mathbf{c}\times\mathbf{a}}{\mathbf{a}\cdot\mathbf{b}\times\mathbf{c}};\ \mathbf{c^*} = \frac{\mathbf{a}\times\mathbf{b}}{\mathbf{a}\cdot\mathbf{b}\times\mathbf{c}}. \tag{2}$$

Each set of atomic planes is labelled with Miller indices (hkl). The vector $\mathbf{H} = h\mathbf{a^*} + k\mathbf{b^*} + l\mathbf{c^*}$ is perpendicular to all the planes in this set, and $d = 1/|\mathbf{H}|$. The crystal's lattice vectors define a unit cell whose volume $V = |\mathbf{a}\cdot\mathbf{b}\times\mathbf{c}|$. If the unit cell is hexagonal, the Miller-Bravais indices $(hkil)$ where $i = -(h+k)$ are often used to make the symmetry of different sets of planes more obvious.

The characteristics of the Bragg reflection from a set of atomic planes (hkl) are given by the structure factor, which is the complex-valued scattering amplitude of one unit cell of the crystal in units of scattering from a single free electron. The structure factor depends on the momentum **q** transferred to the photon by the scattering process. Bragg reflection can occur if **q** is one of the crystal's reciprocal lattice vectors. If the phase term of a plane wave of wave vector **k** is $\exp(-2\pi i\mathbf{k}\cdot\mathbf{r})$, the structure factor at momentum transfer **q** is

$$F(\mathbf{q}) = \sum_j f_j(\mathbf{q}) D_j(\mathbf{q}) \exp\left(2\pi i \mathbf{q}\cdot\mathbf{r}_j\right), \tag{3a}$$

where j denotes a particular atom within the unit cell, $f_j(\mathbf{q})$ is the total atomic scattering factor of the jth atom, $D_j(\mathbf{q})$ is the Debye-Waller factor of the jth atom, and $\mathbf{r}_j = X_j\mathbf{a} + Y_j\mathbf{b} + Z_j\mathbf{c}$ is the position of the jth atom.

At a Bragg reflection from the atomic planes (hkl), $\mathbf{q} = h\mathbf{a^*} + k\mathbf{b^*} + l\mathbf{c^*}$:

$$F(hkl) = \sum_j f_j(hkl) D_j(hkl) \exp\left[2\pi i\left(hX_j + kY_j + lZ_j\right)\right], \tag{3b}$$

Some authors use $\exp(+2\pi i\mathbf{k}\cdot\mathbf{r})$ as the phase term of a plane wave; if this is chosen, the value of $F(hkl)$ is the complex conjugate of that defined above.

The importance of accurate calculations of structure factors in the design of diffracting crystal optics, particularly when used as monochromators, energy analyzers, and phase retarders, should be clear. The angular acceptance and peak reflectivity of a Bragg reflection depend critically on its structure factor, as is shown by many standard texts[26-28]. Phase retarders, which depend on the birefringence of a crystal oriented to an angle close to a Bragg reflection, also require the structure factor of the Bragg reflection to be known for the alignment's precision to be predicted accurately.[29]

2.2 General thermal vibration of the atoms in a crystal

The thermal vibration of the atoms in a crystal enters the calculation of X-ray structure factors through the Debye-Waller factor D_j. In silicon and germanium, the amplitude of this vibration for all atoms is generally assumed to be isotropic and

its temperature dependence is usually characterized by respective Debye temperatures of 543 ± 8 K and 290 ± 5 K[30]. For α quartz, however, this simple assumption fails. Both Le Page *et al*[31] and Kihara[32] agree that the thermal vibrations of both the Si and the O atoms in α quartz are strongly anisotropic. The correct calculation of the Debye-Waller factor for each atom of α quartz therefore requires the use of the thermal displacement ellipsoids, which are explained by Downs[33]. An ellipsoid is characterized by a symmetric 3 × 3 matrix β. The Debye-Waller factor D of an atom with this ellipsoid for a Bragg reflection from the (hkl) atomic planes of the crystal is given by

$$D = \exp[-(\beta_{11}h^2 + \beta_{22}k^2 + \beta_{33}l^2 + 2\beta_{12}hk + 2\beta_{13}hl + 2\beta_{23}kl)]. \quad (4)$$

Often reference works give the thermal ellipsoid matrix β for only one atom of each species. If S is the 3 × 3 matrix of the symmetry operation that transforms the lattice coordinates of this atom into those of another atom in the crystal, the thermal ellipsoid of the second atom is described by the symmetric 3 × 3 matrix

$$\beta' = S\beta S^t, \quad (5)$$

where the superscript t denotes the matrix transpose.

2.3 Nonlinear temperature dependence of crystal structure

For sufficiently small temperature ranges, the temperature dependence of the lattice parameters can be taken as linear, while the temperature dependence of the atomic positions and the Debye-Waller factors can be neglected. However, this is no longer possible even for silicon, germanium, and diamond if the structure factors are to be calculated from the boiling point of liquid nitrogen at atmospheric pressure (77 K) to room temperature, which is the usual operating range of diffracting crystal optics for X-rays. In α quartz, the lattice parameters, atomic positions, and thermal displacement ellipsoids vary highly non-linearly over the temperature range from 13 K to 838 K, which is just below the transition temperature $T_C = 846$ K at which trigonal α (low) quartz transforms into hexagonal β (high) quartz. References are provided in Table 9 of Sutter *et al*[25]. It was found there that the temperature dependence of these quantities followed the general form

$$f(T) = f_0 + P \exp\left(\frac{-Q}{\left\{\ln\left[\frac{T_c}{(T_c - T)}\right]\right\}^n}\right), \quad (6)$$

where the values of the fitting parameters f_0, P, Q, and n are given in Table 10 of Sutter *et al*[25] for a right-handed coordinate system in dextro α quartz in the $z(+)$ setting, which will be explained below. Conversions to other settings are given in Table 8 of that paper. Figure 1 shows how the theoretical fit in Equation (6) matches the experimental data on the lattice parameters a and c of α quartz.

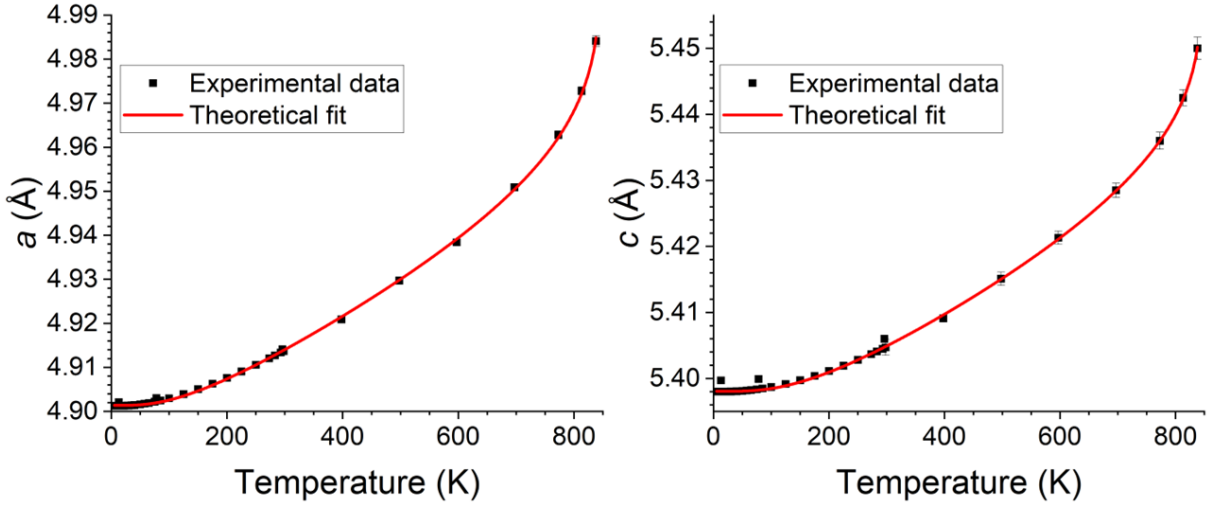

Figure 1: Temperature dependence of the lattice parameters a (left) and c (right) of α quartz over the range 13-838 K. The theoretical fit was obtained by fitting Equation (6) to the experimental data. See text for details.

2.4 Choice of convention for describing a crystal structure

As stated before, some crystal structures may be described in multiple ways. These conventions may differ in one or more of the following. The atomic positions to be used to determine the structure factor will differ accordingly. If the axes differ, then so too will the assignment of Miller indices to the crystal's atomic planes.

1.) Placement of the coordinate system's origin. The two choices available for crystal structures of the $Fd\bar{3}m$ space group, which include silicon, germanium, and diamond, have already been mentioned. In α quartz, there are also different choices that can be made. The origin is always placed at the intersection of the **c** axis, which is the 3-fold screw axis, with one of the three 2-fold axes perpendicular to **c**, on which the Si atoms are located. However, Donnay and Le Page[22] place the origin so that the first Si atom is at coordinates $(u, 0,0)$, while the International Tables for Crystallography[5] place the origin so that the first Si atom is at $\left(u, 0, \frac{2}{3}\right)$ if the screw axis is left-handed and at $\left(u, 0, \frac{1}{3}\right)$ if the screw axis is right-handed.

2.) Right- or left-handedness of the lattice coordinate system. This is particularly an issue for chiral crystal structures, which may exist in either of two mirror-imaged forms that cannot be superimposed on each other and therefore also have a handedness. α quartz crystals possess such a structure. The handedness of the coordinate system may be chosen to match that of the crystal structure, or else the coordinate system may be given the same handedness independently of that of the crystal structure.

3.) Definition of the handedness of a chiral crystal structure. This causes much confusion in the treatment of α quartz and was therefore discussed in detail by Donnay and Le Page[22], and also by Glazer[24]. "Dextro" α quartz rotates the polarization of light clockwise as seen by an observer looking upstream. However, although "dextro" is Latin for "right," the screw axis is actually *left*-handed. Similarly, "laevo" α quartz rotates the polarization of light counterclockwise as seen by an observer looking upstream, yet although "laevo" is Latin for "left," the screw axis is actually *right*-handed.

4.) Orientation of the lattice coordinate axes relative to the atoms of the crystal structure. A few examples of this are found

   a.) in certain crystals with orthorhombic structures such as topaz[34], which belongs to the space group $Pnma$, and potassium acid phthalate[35], which belongs to the space group $Pca2_1$. These two crystals are included in the comprehensive list of diffractive elements in the *X-Ray Data Booklet*[36]. A non-standard setting $Pbnm$ can be defined for the space group $Pnma$ by relabeling the lattice vectors **a**, **b**, and **c** as **c**, **a**, and **b**, respectively. Similarly, a non-standard setting $P2_1ab$ can be defined for the space group $Pca2_1$ by relabeling the lattice vectors **a**, **b**, and **c** as **b**, **c**, and **a**, respectively.

   b.) in monoclinic crystals, where one of the lattice vectors is perpendicular to the other two. This may be labelled either **b** or **c**, with Parthé and Gelato[20] preferring the former. Muscovite, recently proposed for making spherically bent X-ray energy analyzers[37], belongs to this group.

   c.) finally, in α quartz. Although the **a** and **b** lattice vectors are always defined parallel to two of the three 2-fold axes, a rotation of the lattice coordinate system by 180° about **c** switches the setting between the "obverse" (*r*) and "reverse" (*z*). In the obverse setting, the $(10\bar{1}1)$ Bragg reflection is stronger than the $(10\bar{1}\bar{1})$ Bragg reflection, and the $(30\bar{3}1)$ Bragg reflection is much stronger than the $(30\bar{3}\bar{1})$ Bragg reflection[24]. Atomic planes in α quartz that are assigned the $(hkil)$ Miller-Bravais indices in the obverse setting are assigned the $(\overline{hkil})$ indices in the reverse setting. Knowing this and the symmetry relations of the α quartz crystal structure, one finds that in the reverse setting the $(10\bar{1}1)$ Bragg reflection is weaker than the $(10\bar{1}\bar{1})$ Bragg reflection, and the $(30\bar{3}1)$ Bragg reflection is much weaker than the $(30\bar{3}\bar{1})$ Bragg reflection. If a right-handed coordinate system is chosen, Donnay and Le Page[22] have labelled the obverse settings as $r(-)$ for dextro α quartz and $r(+)$ for laevo α quartz, and they have labelled the reverse settings as $z(+)$ for dextro α quartz and $z(-)$ for laevo α quartz. For a left-handed coordinate system, the names of the settings for dextro and laevo α quartz would be switched.

5.) Type of unit cell. Crystal structures that have trigonal systems and whose space groups have labels beginning with R, such as sapphire and lithium niobate, may be described with either a rhombohedral or a hexagonal unit cell, although the hexagonal unit cell is much more common in practice. More complex is the case of a triclinic

crystal structure, which has no symmetry operations other than translations to impose any choice of lattice vectors **a**, **b**, and **c**. There are only necessary constraints on the angles between them[38]. The problem of choosing a standard unit cell that would permit different crystallographers to compare their data on the same crystal structure was by no means trivial. This problem was solved by Niggli, who first defined a unique unit cell that was reduced; that is, based on the three shortest vectors of the lattice[39]. The process of determining this cell for any crystal structure was then put on a systematic basis by Santoro and Mighell[40]. However, other unit cells may still be encountered in the literature. For instance, centered monoclinic crystal structures were still being described by non-standard unit cells decades after the above papers were published[41].

3. COMPUTATION AND CODING

Evidently the accurate and rapid computation of X-ray structure factors in crystals, which is vital for the design of diffractive X-ray optics, needs to account for the diversity of temperature dependencies and descriptions of the many crystal structures that may be encountered. Moreover, even when a widely respected authority speaks in favor of a particular description for a given crystal structure, there may be valid reasons to use a different one. Once again, α quartz provides an example. As mentioned before, if one is guided by the International Tables for Crystallography[5], then in a right-handed coordinate system, the origin of the α quartz structure should be placed so that the first silicon atom is at coordinates $\left(u, 0, \frac{2}{3}\right)$ in the dextro structure (space group $P3_221$) and $\left(u, 0, \frac{1}{3}\right)$ in the laevo structure (space group $P3_121$). However, at 846 K, the dextro α quartz structure transitions to left-screw β quartz (space group $P6_222$), which according to the International Tables for Crystallography should have its first silicon atom at $\left(\frac{1}{2}, 0,0\right)$. Likewise, the laevo α quartz structure transitions to right-screw β quartz (space group $P6_422$). Again, the International Tables for Crystallography would lead one to place the first silicon atom at $\left(\frac{1}{2}, 0,0\right)$. This leads to a discontinuity in the *c* coordinate of the first silicon atom across the transition from α quartz to β quartz. Donnay and Le Page's choice of $(u, 0,0)$ as the coordinates of the first silicon atom in both dextro and laevo α quartz avoids this problem and was therefore adopted by Glazer[24] despite the high standing of the International Tables of Crystallography.

The software package *PyCSFex* does not attempt to take sides in these longstanding debates among crystallographers, except to require that a right-handed coordinate system be used in all cases. Other than that, it allows individual users to describe their crystals in the way that is most comfortable for them. It aims for the easiest possible application to new crystals and for the fastest possible calculation of large numbers of structure factors. Several strategies were employed to reach these goals. The first was the choice of the Python 3 programming language for writing the code. Python 3 is widely used and understood, and it makes *PyCSFex* compatible with *OASYS*[18] and *SRW*[19] as well as allowing it to function independently. The second was the modular architecture of the code. The modules of *PyCSFex* are separated into three clearly defined categories:

1.) Core files. These are meant to be stable modules that users should not need to alter. They are all the files located in the folder `Structure_Factor_Calculator` and in addition the Excel spreadsheet `Form_factor_coefficients.xlsx`, which contains the coefficients for calculating non-anomalous X-ray atomic scattering factors according to the five-Gaussian fit of Waasmaier and Kirfel[42]. `Structure_Factor_Calculator` contains the following:

   a.) A folder `xrpy` that contains modules for the calculation of atomic X-ray scattering and absorption. These are based on the previous work of Brennan and Cowan[43].

   b.) The definition of a class `Atom` for descriptions of each atom.

   c.) The definition of a class `Diff_Environment` for basic calculations of Bragg reflection.

   d.) A list of common physical constants.

   e.) Basic methods for vector calculations.

   f.) Methods for reading the coefficients in `Form_factor_coefficients.xlsx`.

   g.) The final calculation of the structure factor according to Equation (3b).

2.) Material files. These are all the files located in the folder `general_crystals`. The only files here that must remain unchanged are `general_crystal.py`, which constructs an object with basic attributes and methods that apply to all crystal structures, and of course `__init__.py`. Other files may be added by the user. Model material files are provided in the Github distribution. A detailed explanation is provided in the *PyCSFex* paper[25]. In each material file, a class for the description of a single crystal structure under a specific model of temperature dependencies and a chosen convention is defined. The creation of an object of this class requires three arguments: temperature in K, the Miller indices of the diffracting atomic planes, and the photon energy in eV. Different thermal models and different conventions for the same crystal structure can be easily accommodated in separate material files.

3.) Scripts. These are all the files located in the folder `Examples`. Several model scripts are available in the Github distribution. Examples of the outputs of some representative scripts are provided in the *PyCSFex* paper; a selection of these will be shown here. Users may apply the procedures in the core and material files to write their own scripts, which they may freely add to the `Examples` folder.

The third strategy was to avoid redundant calculations. For example, temperature-dependent parameters such as lattice parameters, atomic positions, and thermal vibrations are recalculated only when the temperature is changed. Also, each class has a method to update its attributes when required, thus avoiding the need to create a new object of that class with the new attributes.

4. RESULTS

In the following, dextro α quartz in the $z(+)$ setting is assumed. If laevo α quartz in the $z(-)$ setting is assumed, the indices $(hkil)$ are replaced by $(\overline{hkil})$. A right-handed coordinate system is always chosen.

4.1 Comparison of isotropic and anisotropic models of thermal vibration in α quartz

The anisotropic thermal vibration of the atoms in α quartz has already been mentioned and the method for calculating the Debye-Waller factors from its characteristic thermal ellipsoids has been explained. However, the mathematical complexity of thermal ellipsoids makes it worthwhile to see how much error would be introduced to the structure factors if the thermal vibration were treated as isotropic. One simple approximation is an isotropic Debye model with a Debye temperature of 470 K as given by Gray[44]. The four Bragg reflections $(10\bar{1}1)$, $(10\bar{1}\bar{1})$, $(30\bar{3}1)$, and $(30\bar{3}\bar{1})$ are interesting because they cover a wide range of strengths from very intense to very weak. Furthermore, at the transition from α quartz to β quartz, the first pair of these reflections becomes symmetrically equivalent, so that their structure factors become equal. The same is true for the second pair of these reflections. A set of calculations was therefore performed using two separate material files, one for the isotropic approximation and the other for the full anisotropic treatment.

Figure 2 shows the results of calculations with *PyCSFex* with 10 keV X-rays. For the $(10\bar{1}1)$ and $(10\bar{1}\bar{1})$ Bragg reflections, the isotropic model of thermal vibration consistently gives higher estimates of the reflection's strength. The discrepancy remains below 1% up to 530 K for $(10\bar{1}1)$ and up to 412 K for $(10\bar{1}\bar{1})$, but as the temperature increases further, the isotropic model deviates steadily more from the anisotropic model. At the highest measured temperature of 838 K, the discrepancy has increased to 5.3%. This is still small, but for the very weak reflection $(30\bar{3}1)$, the disagreement between the two thermal models is very large, especially above 600 K. It is noteworthy that in both thermal models the structure factor of $(30\bar{3}1)$ passes through a minimum, though in the isotropic model the minimum is at 562 K, while in the anisotropic model the minimum is at 536 K. The stronger reflection $(30\bar{3}\bar{1})$ is much less affected by the difference in the thermal models, the largest discrepancy being only 4.3% at 643 K. Here, however, the isotropic model provides a lower estimate of the reflection's strength than the anisotropic model.

4.2 Search for Bragg reflections in α quartz that backscatter X-rays of specified energy

To determine the Bragg reflection that most nearly approaches the ideal condition of backscattering for a crystal energy analyzer to achieve its highest possible resolution, a large number of Bragg reflections will in general need to be searched. *PyCSFex* allowed this to be done for dextro α quartz over all temperatures from 20 K to 600 K. Table 2 shows the reflections that can backscatter X-rays at the Mo $K\alpha_1$ energy of 17.479 keV, and Table 3 lists the reflections that can backscatter X-rays at the Cu $K\alpha_1$ energy of 8.048 keV. T_b is the temperature at which each set of diffracting atomic planes $(hkil)$ has a spacing equal to exactly half the X-ray wavelength, which is the required condition for backscattering as shown by Equation 1. R_{pk} is the peak reflectivity, ΔE_{FWHM} is the full width at half maximum of the curve of reflectivity

versus energy, and mK/meV is the change in temperature in millikelvin required to change the backscattered X-ray energy by +1 meV. Each of the atomic planes $(hkil)$ is one of six symmetrically related planes that will all have the same diffractive properties: $(hkil)$, $(ihkl)$, $(kihl)$, $(hik\bar{l})$, $(khi\bar{l})$, and $(ikh\bar{l})$.

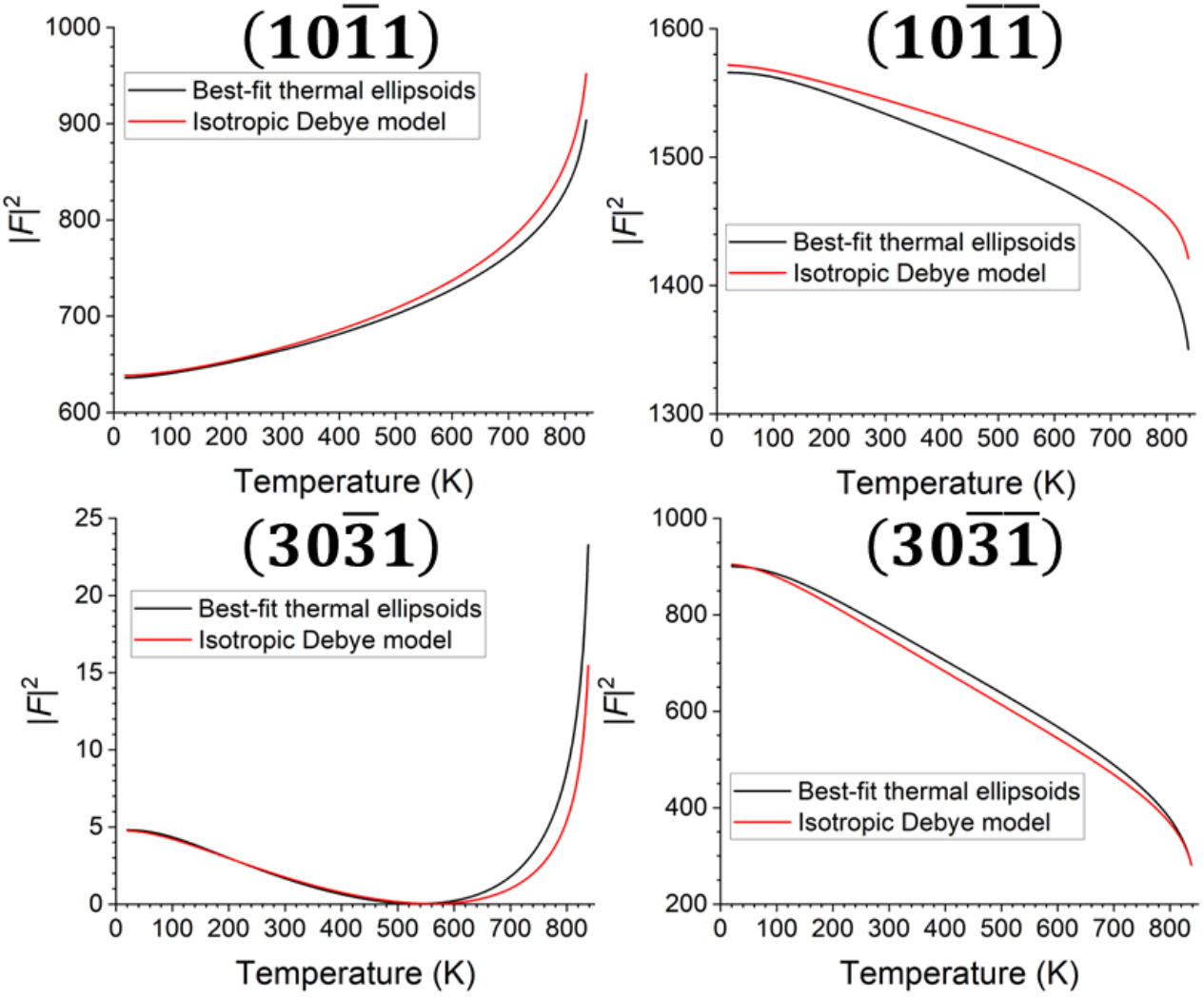

Figure 2: Temperature dependence from 20 K to 838 K of the squared magnitude of the structure factors of the $(10\bar{1}1)$, $(10\bar{1}\bar{1})$, $(30\bar{3}1)$, and $(30\bar{3}\bar{1})$ Bragg reflections of dextro α quartz in the $z(+)$ setting with X-rays of 10 keV energy.

Table 2: Backscattering reflections of dextro α quartz in the $z(+)$ setting for Mo $K\alpha_1$ X-rays (17.479 keV). See text for details.

$(hkil)$	T_b (K)	R_{pk}	ΔE_{FWHM} (meV)	mK/meV
$(\bar{1}\bar{1}\ 0\ 11\ \bar{6})$	70	0.85	2.29	−15.9
$(\bar{1}\bar{1}\ 0\ 11\ 6)$	70	0.79	1.64	−15.9
$(\bar{7}\ 2\ 5\ \bar{1}\bar{3})$	222	0.63	0.89	−6.7
$(\bar{7}\ 2\ 5\ 13)$	222	0.70	1.08	−6.7
$(\bar{1}\bar{2}\ 0\ 12\ 0)$	304	0.15	0.26	−3.9

$(\overline{13}\ 5\ 8\ \overline{5})$	420	0.52	0.63	−3.6
$(\overline{13}\ 5\ 8\ 5)$	420	0.29	0.36	−3.6
$(\overline{8}\ \overline{5}\ 13\ 5)$	420	0.32	0.36	−3.6
$(\overline{13}\ 3\ 10\ \overline{3})$	434	0.32	0.38	−3.5
$(\overline{13}\ 3\ 10\ 3)$	434	0.27	0.34	−3.5
$(\overline{10}\ \overline{3}\ 13\ \overline{3})$	434	0.34	0.38	−3.5
$(\overline{10}\ \overline{3}\ 13\ 3)$	434	0.28	0.34	−3.5
$(\overline{12}\ 0\ 12\ \overline{1})$	441	0.71	1.16	−3.4

Table 3: Backscattering reflections of dextro α quartz in the $z(+)$ setting for Cu Kα$_1$ X-rays (8.048 keV). See text for details.

$(\boldsymbol{hkil})$	$\boldsymbol{T_b}$ **(K)**	$\boldsymbol{R_{pk}}$	$\boldsymbol{\Delta E_{FWHM}}$ **(meV)**	**mK/meV**
$(\bar{6}\ 2\ 4\ \bar{2})$	246	0.61	8.48	−9.5
$(\bar{6}\ 2\ 4\ 2)$	246	0.83	17.96	−9.5
$(\bar{4}\ \bar{2}\ 6\ \bar{2})$	246	0.67	8.48	−9.5
$(\bar{5}\ 0\ 5\ \bar{3})$	364	0.40	4.34	−8.6

5. CONCLUSIONS

Optics designers wishing to build diffractive X-ray optics such as monochromators, phase retarders, and energy analyzers must accurately calculate the X-ray structure factors of a wide variety of crystals. Even though the cubic crystals of silicon, germanium, and diamond remain by far the most popular materials for such optics because of their favorable thermal and mechanical properties, several trigonal crystals have also attracted notice for specific applications such as high-resolution energy analyzers. Sapphire, lithium niobate, and especially α quartz are being evaluated for this purpose. Of these, the material in which synthetic crystals of the best quality are available is α quartz, which therefore has already been used in experimental condensed matter studies. The use of still other crystals for X-ray energy analysis, such as topaz (orthorhombic), potassium acid phthalate (orthorhombic), and muscovite (monoclinic), has been recorded in the literature as well. However, neither the modeling of the temperature dependence nor the choice of convention used to describe the crystal structure is consistently made clear in current structure factor calculations that are aimed at X-ray optics designers. As the discussion of the obverse and reverse settings of α quartz proves, such lack of clarity can lead to gross errors. A new Python 3 package named *PyCSFex* has been published so that users can choose their own preferred thermal models and conventions, because even though much work has gone into the standardization of descriptions of crystal structures, some users may still have sound reasons to select a non-standard description. *PyCSFex* consists of a set of stable core files that are not changed, a set of material files written by the user to describe each crystal structure, and a set of scripts written by the user that apply the core and material files to carry out the desired calculations. Different thermal models and descriptions of the same crystal structure can be written in separate material files, thus minimizing the possibility of confusion. Examples of structure factor calculations on α quartz, which has an especially complex and challenging crystal structure, have been provided to demonstrate how *PyCSFex* can help solve practical problems in X-ray diffractive optics design.

ACKNOWLEDGMENTS

This work was carried out with the support of Diamond Light Source Ltd. We thank Diamond Light Source Ltd for the summer placement of one of us (JP). We especially thank Kawal Sawhney, head of Diamond's Optics and Metrology Group, for supporting us. Graeme Winter, Principal Software Scientist of Life Sciences at Diamond, took the time to explain *cctbx* and especially its use of standardized descriptions of crystal structures. Sean Brennan freely gave us his Python 3 version of his program *abs*, which calculates the anomalous dispersion, Compton, and Rayleigh corrections to X-ray atomic scattering factors. Finally, Taishun Manjo of SPring-8's CSRR Precision Spectroscopy Division helped to write material files for silicon, germanium, and diamond.

REFERENCES

[1] Glassbrenner. C. J. and Slack, G. A., "Thermal conductivity of silicon and germanium from 3°K to the melting point," *Phys. Rev.* **134**(4A), A1058-A1069 (1964).
[2] Gibbons, D. F., "Thermal expansion of some crystals with the diamond structure," *Phys. Rev.* **112**(1), 136-140 (1958).
[3] Stoupin, S. and Shvyd'ko, Y. V., "Ultraprecise studies of the thermal expansion coefficient of diamond using backscattering X-ray diffraction," *Phys. Rev. B* **83**(10), 104102 (2011).
[4] Touloukian, Y. S., Powell, R. W., Ho, C. Y. and Klemens, P. G. [Thermophysical Properties of Matter: The TPRC Data Series], Vol. 2, "Thermal Conductivity – Nonmetallic Solids," pp. 174-182. IFI/Plenum, New York (1970).
[5] International Tables for Crystallography, Vol. A, "Space-group symmetry," second online edition, edited by M. I. Aroyo (2016).
[6] Bergmann, U. and Cramer, S. P., "A high-resolution large-acceptance analyzer for X-ray fluorescence and Raman spectroscopy," *Proc. SPIE* **3448**, 198-209 (1998).
[7] Baron, A. Q. R., "Introduction to high-resolution inelastic X-ray scattering," in [Synchrotron Light Sources and Free-Electron Lasers], edited by E. J. Jaeschke, S. Khan, J. R. Schneider, and J. B. Hastings, Springer International Publishing, Switzerland, pp. 1643-1757 (2016). See also https://arxiv.org/abs/1504.01098.
[8] Sutter, J. P., Alp, E. E., Hu, M. Y., Lee, P. L., Sinn, H., Sturhahn, W., Toellner, T. S., Bortel, G. and Colella, R., "Multiple-beam X-ray diffraction near exact backscattering in silicon," *Phys. Rev. B* **63**(9), 094111 (2001).
[9] Yavaş, H., Sutter, J. P., Gog, T., Wille, H.-C., and Baron, A. Q. R., "New materials for high-energy-resolution X-ray optics," *MRS Bulletin* **42**(6), 424-429 (2017).
[10] Laudise, R. A., "Hydrothermal synthesis of crystals," *Chem. Eng. News* **65**(39), 30-43 (1987).
[11] Sutter, J. P., Baron, A. Q. R., Ishikawa, T. and Yamazaki, H., "Examination of Bragg backscattering from crystalline quartz," *J. Phys. Chem. Solids* **66**(12), 2306-2309 (2005).
[12] Sutter, J. P., Baron, A. Q. R., Miwa, D., Nishino, Y., Tamasaku, K. and Ishikawa, T., "Nearly perfect large-area quartz: 4 meV resolution for 10 keV photons over 10 cm^2," *J. Synchrotron Rad.* **13**(3), 278-280 (2006).
[13] Imai, Y., Yoda, Y., Zhang, X. and Kikuta, S., "Backscattering of α-quartz (0 6 10) for 14.4 keV Mössbauer photons," *AIP Conf. Proc.* **879**, 930-932 (2007).
[14] Hönnicke, M. G., Huang, X., Cusatis, C., Koditwuakku, C. N. and Cai, Y. Q., "High-quality quartz single crystals for high-energy-resolution inelastic X-ray scattering analyzers," *J. Appl. Cryst.* **46**(4), 939-944 (2013).
[15] Honnicke, M. G., Bianco, L. M., Ceppi, S. A., Cusatis, C., Huang, X., Cai, Y. Q. and Stutz, G. E., "Construction of a quartz spherical analyzer: application to high-resolution analysis of the Ni Kα emission spectrum," *J. Appl. Cryst.* **49**(5), 1443-1453 (2016).
[16] Said, A. H., Gog, T., Wieczorek, M., Huang, X., Casa, D., Kasman, E., Divan, R. and Kim, J. H., "High-energy-resolution diced spherical quartz analyzers for resonant inelastic X-ray scattering," *J. Synchrotron Rad.* **25**(2), 373-377 (2018).
[17] Kim, J., Casa, D., Said, A., Krakora, R., Kim, B. J., Kasman, E., Huang, X. and Gog, T., "Quartz-based flat-crystal resonant inelastic X-ray scattering spectrometer with sub-10 meV energy resolution," *Sci. Rep.* **8**, 1958 (2018).
[18] Sanchez del Rio, M. and Rebuffi, L, "OASYS: A software for beamline simulations and synchrotron virtual experiments," *AIP Conf. Proc.* **2054**, 060081 (2019).
[19] Chubar, O. and Elleaume, P., "Accurate and efficient computation of synchrotron radiation in the near field region," in [Proceedings of EPAC '98, Sixth European Particle Accelerator Conference], 22-26 June 1998,

Stockholm, Sweden, edited by S. Myers, L. Liljeby, C. Petit-Jean-Genaz, J. Poole, and K.-G. Rensfelt, pp. 1177-1179. Institute of Physics, Bristol (1998).
[20] Parthé, E. and Gelato, L. M., "The standardization of inorganic crystal-structure data," *Acta Cryst. A* **40**(3), 169-183 (1984).
[21] Grosse-Kunstleve, R. W., Sauter, N. K., Moriarty, N. W. and Adams, P. D., "The *Computational Crystallography Toolbox*: crystallographic algorithms in a reusable software framework," *J. Appl. Cryst.* **35**(1), 126-136 (2002). The *Computational Crystallography Toolbox* (*cctbx*) is available at https://github.com/cctbx/cctbx_project.
[22] Donnay, J. D. H. and Le Page, Y., "The vicissitudes of the low-quartz crystal setting or the pitfalls of enantiomorphism," *Acta Cryst. A* **34**(4), 584-594 (1978).
[23] Huang, X.-R., Gog, T., Kim, J., Kasman, E., Said, A. H., Casa, D. M., Wieczorek, M., Hönnicke, M. G., and Assoufid, L., "Correct interpretation of diffraction properties of quartz crystals for X-ray optics applications," *J. Appl. Cryst.* **51**(1), 140-147; **51**(3), 966-967 (2018).
[24] Glazer, A. M., "Confusion over the description of the quartz structure yet again," *J. Appl. Cryst.* **51**(3), 915-918 (2018).
[25] Sutter, J. P., Pittard, J., Filik, J. and Baron, A. Q. R., "Calculating temperature-dependent X-ray structure factors of α quartz with an extensible Python 3 package," *J. Appl. Cryst.* **55**(4), 1011-1028 (2022).
[26] Zachariasen, W. H. [Theory of X-ray Diffraction in Crystals], John Wiley & Sons, New York (1945).
[27] Batterman, B. W. and Cole, H., "Dynamical diffraction of X-rays by perfect crystals," *Rev. Mod. Phys.* **36**(3), 681-717 (1964).
[28] Authier, A. [International Tables for Crystallography (first online edition)], Vol. B, *Reciprocal Space*, Chapter 5.1, pp. 534-551, International Union of Crystallography, Chester (2006).
[29] Giles, C., Malgrange, C., Goulon, J., de Bergevin, F., Vettier, C., Dartyge, E., Fontaine, A., Giorgetti, C. and Pizzini, S., "Energy-dispersive phase plate for magnetic circular dichroism experiments in the X-ray range," *J. Appl. Cryst.* **27**(3), 232-240 (1994).
[30] Batterman, B. W. and Chipman, D. R., "Vibrational amplitudes in germanium and silicon," *Phys. Rev.* **127**(3), 690-693 (1962).
[31] Le Page, Y., Calvert, L. D. and Gabe, E. J., "Parameter variation in low-quartz between 94 and 298 K," *J. Phys. Chem. Solids* **41**(7), 721-725 (1980).
[32] Kihara, K., "An X-ray study of the temperature dependence of the quartz structure," *Eur. J. Mineral.* **2**(1), 63-77 (1990).
[33] Downs, R. T., "Analysis of harmonic displacement factors," *Rev. Mineral. Geochem.* **41**(1), 61-87 (2000).
[34] Komatsu, K., Kuribayashi, T. and Kudoh, Y., "Effect of temperature and pressure on the crystal structure of topaz, $Al_2SiO_4(OH,F)_2$," *J. Mineral. Petrological Sci.* **98**(5), 167-180 (2003).
[35] Okaya, Y., "The crystal structure of potassium acid phthalate, $KC_6H_4COOH.COO$," *Acta Cryst.* **19**(6), 879-882 (1965).
[36] Underwood, J. H., "Multilayers and crystals," in [X-Ray Data Booklet], third edition, Section 4.1 B, Center for X-Ray Optics and Advanced Light Source, Lawrence Berkeley National Laboratory, California (2009). https://xdb.lbl.gov/Section4/Sec_4-1.html, Table 4-1.
[37] Joseph, E. S., Jahrman, E. P. and Seidler, G. T., "Spherically bent mica analyzers as universal dispersing elements for X-ray spectroscopy," *X-Ray Spectroscopy* **49**(4), 493-501 (2020).
[38] Foadi, J. and Evans, G., "On the allowed values for the triclinic unit-cell angles," *Acta Cryst. A* **67**(1), 93-95 (2011).
[39] Niggli, P., "Krystallographie und Strukturtheoretische Grundbegriffe," *Handbuch der Experimentalphysik*, Vol. 7, Part 1, Akademische Verlagsgesellschaft, Leipzig (1928).
[40] Santoro, A. and Mighell, A. D., "Determination of reduced cells," *Acta Cryst. A* **26**(1), 124-127 (1970).
[41] Mighell, A. D., "Conventional cells – the last step toward general acceptance of standard conventional cells for the reporting of crystallographic data," *J. Res. Natl. Inst. Stand. Technol.* **107**(4), 373-377 (2002).
[42] Waasmaier, D. and Kirfel, A., "New analytical scattering-factor functions for free atoms and ions," *Acta Cryst. A* **51**(3), 416-431 (1995).
[43] Brennan, S. and Cowan, P. L., "A suite of programs for calculating X-ray absorption, reflection, and diffraction performance for a variety of materials at arbitrary wavelengths," *Rev. Sci. Instrum.* **63**(1), 850-853 (1992).
[44] Gray, D. E. [American Institute of Physics Handbook], McGraw-Hill, New York (1957).